Migration velocity analysis by double path-integral migration

J. Schleicher* and J. C. Costa†

*Dept. of Applied Math., IMECC-UNICAMP, CP 6065, 13083-859 Campinas (SP), Brazil

†Faculty of Geophysics, Federal University of Pará, 66.075-110, Belém (PA), Brazil

This paper was prepared for presentation at the 11th International Congress of The Brazilian Geophysical Society held in Salvador, Brazil, August 24-28, 2009.

Abstract

The idea of path-integral imaging is to sum over the migrated images obtained for a set of migration velocity models. Those velocities where common-image gathers align horizontally are stationary, thus favoring these images in the overall stack. In this way, the overall image forms with no knowledge of the true velocity model. However, the velocity information associated with the final image can be determined in the process. By executing the path-integral imaging twice, weighting one of the stacks with the velocity value, the stationary velocities that produce the final image can then be extracted by a division of the two images. A numerical example demonstrates that quantitative information about the migration velocity model can be determined by double path-integral migration.

Introduction

The quality of seismic images of the earth's interior is strongly dependent on the available velocity model. Keydar (2004) and Landa (2004) have proposed a path-integral approach to seismic imaging in order to overcome this dependency on the knowledge of a velocity model. The idea of path-integral imaging is to sum over the migrated images obtained for a set of migration velocity models. Those velocities where common-image gathers align horizontally are stationary, thus favoring these images in the overall stack. In this way, the overall image forms with no need to know the true velocity model.

Keydar (2004) applied the technique to inversion by homeomorphic imaging. Landa (2004) extended the idea to time migration. He proposed to obtain the final subsurface seismic image by a summation of time-migrated images with a representative sample of all possible velocity models. The constructive and destructive interference of the elementary signals contributed by each model produces an image that converges towards the one which would be obtained by a migration using the stationary velocity field. First applications of path-summation imaging in depth migration were presented by Landa et al. (2005) and Shtivelman and Keydar (2005).

Landa et al. (2006) discuss path-summation imaging in more conceptual and theoretical detail. They stress that there are three essential conditions for path-summation imaging to be successful: (1) the argument of the path integral is chosen adequately; (2) the integration is carried out over a representative sample of all possible trajectories; (3) a properly designed weight function is applied in the multipath summation. A successful weight function was discussed by Keydar et al. (2008).

Multipath summation eliminates the need to construct a migration velocity model before imaging. However, this asset turns into a drawback when the actual velocity model is needed. In this paper, we show how the multipath summation can be modified to extract a meaningful velocity model together with the final image. By executing the path-integral imaging twice and weighting one of the stacks with the used velocity value, the stationary velocities that produce the final image can then be extracted by a division of the two images. A numerical example demonstrates that information about the migration velocity can be extracted successfully from path-integral migration.

Multipath-summation time migration

In the notation of Landa et al. (2006), the multipath time-migration operator can be written as

$$V_W(\mathbf{x}) = \int d\alpha\; w(\mathbf{x},\alpha) \int d\xi \int dt\; U(t,\xi)\delta(t-t_d(\xi,\mathbf{x},\alpha))\;, \tag{1}$$

where V_W is the resulting time-migrated image at an image point with coordinates $\mathbf{x} = (x,\tau)$, x being lateral distance and τ vertical time. In integral (1), $U(t,\xi)$ denotes a seismic trace at coordinate ξ in the seismic data, and $t_d(\xi,\mathbf{x},\alpha)$ is a set of stacking surfaces corresponding to a set of possible velocity models α. Note that generally, the migration velocity α is a function of the position $\mathbf{x}$ of the image point, i.e., $\alpha = \alpha(\mathbf{x})$. There are several possible choices for weight function $w(\mathbf{x},\alpha)$. We opted for an exponential weight function of the form

$$w(\mathbf{x},\alpha) = \exp[-P(\mathbf{x},\alpha)/\sigma^2]\;, \tag{2}$$

where $P(\mathbf{x},\alpha)$ is the squared average of the absolute value of the local event slopes in the common-image gather (CIG) at $\mathbf{x}$. We estimate the local event slopes using corrected least-square plane-wave filters (Schleicher et al., 2009). Parameter σ adjusts the half-width of the Gaussian bell function. We chose $\sigma = 0.1\Delta\tau/\Delta x$.

Integrals of the form of equation (1) with an exponential weight of the type of equation (2) have their main contribution from the point α_0 at which the function in the exponent has its maximum value. Clearly, in our case, the maximum value is reached at $P = 0$. Hence, the stationary value α_0 corresponds to the best possible migration velocity. Using

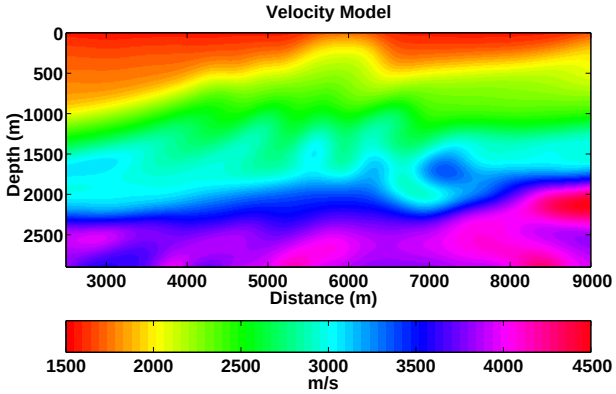

Figure 1: Marmousoft velocity model.

Laplace's method, integral (1) can be asymptotically evaluated (see also Landa et al., 2006) to yield

$$V_W(\mathbf{x}) \approx \sqrt{\frac{2\pi\sigma^2}{P''(\alpha_0)}} Q_0(\mathbf{x}, \alpha_0) \ , \tag{3}$$

where $P''(\alpha_0)$ denotes the second derivative of the squared local slope mean P as a function of the varying migration velocity α. Moreover, $Q_0(\mathbf{x}, \alpha_0)$ denotes the desired migration result with the stationary migration velocity α_0.

Equation (3) justifies the claim that the result of a multipath summation produces a migrated image. In fact, we see that the result of multipath summation is directly proportional to the desired migration result.

Double multipath summation

The observation that the summation result is proportional to the desired image has another important consequence. It implies that the use of a slightly modified weight function

$$\tilde{w}(\mathbf{x}, \alpha) = \alpha \exp(-P((\mathbf{x}, \alpha)/\sigma^2) \ , \tag{4}$$

will lead to a slightly modified migration result,

$$\tilde{V}_W(\mathbf{x}) \approx \alpha_0 \sqrt{\frac{2\pi\sigma^2}{P''(\alpha_0)}} Q_0(\mathbf{x}, \alpha_0) \ . \tag{5}$$

In other words, results (3) and (5) differ only by a constant factor, this factor being the true migration velocity at $\mathbf{x}$. This readily suggests that the migration velocity can be extracted from such a procedure by simply dividing the two migration results (3) and (5), i.e.,

$$\alpha_0(\mathbf{x}) \approx \tilde{V}_W(\mathbf{x}) \big/ V_W(\mathbf{x}) \ . \tag{6}$$

This idea of extracting quantities from multiple stacks has already been previously discussed in the framework of Kirchhoff migration (Bleistein, 1987; Tygel et al., 1993).

Numerical Examples

We have applied the above technique of velocity model building to the Marmousoft data (Billette et al., 2003). These data were constructed by Born modeling in a smoothed version of the Marmousi model. The true Marmousoft velocity model is depicted in Figure 1.

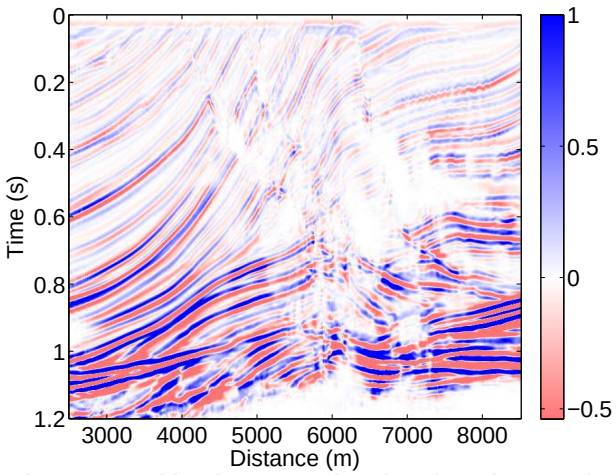

Figure 2: Multipath-summation time imaging result.

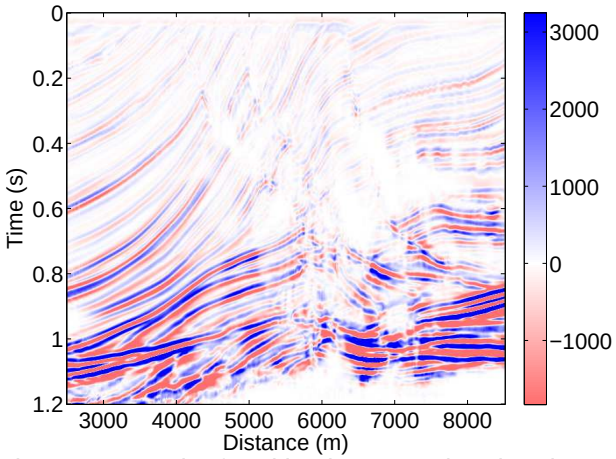

Figure 3: Result of multipath-summation time imaging with additional velocity weight.

We carried out a multipath-summation time migration using constant migration velocities between 1.4 km/s and 4.2 km/s in intervals of 25 m/s. This velocity sampling is sufficiently dense to satisfy condition 2 from the introduction. The resulting stacked migrated image is shown in Figure 2. We see that the multipath-summation approach produces a very nice image that exhibits the main structures of the Marmousi model, even though the central part of the image is not perfectly recovered. This is due to the intrinsic limitations of time migration rather than those of multipath summation. In this region, the image gathers could not be flattened by time migration. Thus, there is no stationary point in integral (1), i.e., no constructive interference to form an image.

Simultaneously, we carried out a second multipath-summation time migration using the same velocity values. It differed from the first one only by the use of the migration velocity as an additional weight factor in the stack. The resulting migrated image is shown in Figure 3. It looks quite similar to the unweighted stack result. As the only difference, we immediately note the increasing amplitudes with depth in comparison to Figure 2, indicating the increasing velocities that the amplitudes of Figure 3 carry. As indicated by the colorbar, the migrated amplitudes are in the range of seismic velocities.

The division of the images of Figures 2 and 3 results in a

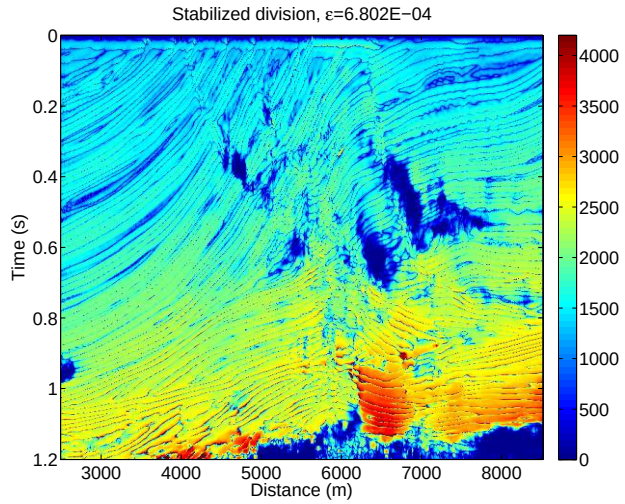

Figure 4: Velocities extracted by stabilized division.

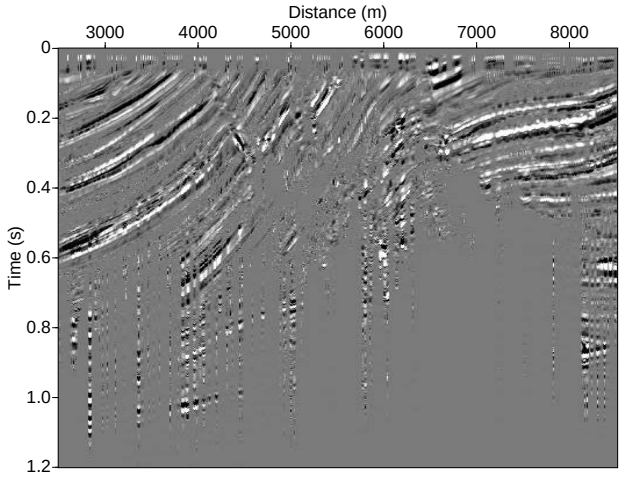

Figure 5: Time migration using velocities extracted by stabilized division.

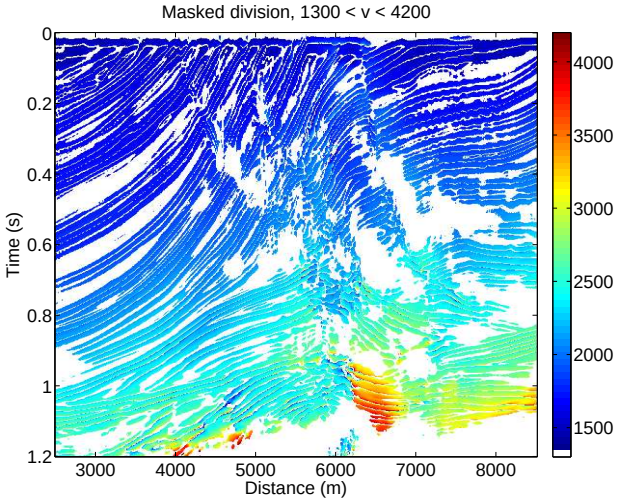

Figure 6: Velocities extracted by masked division.

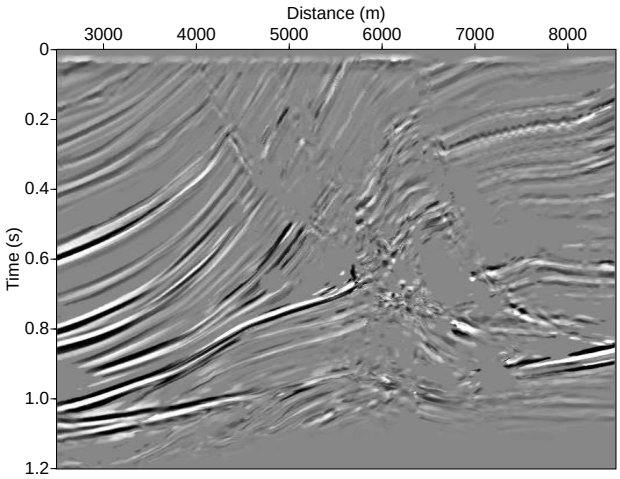

Figure 7: Time migration using velocities extracted by masked division.

migration velocity model. Figure 4 shows the result when the division is stabilized by adding a fraction of the maximum amplitude to the denominator. We recognize that the overall trend of the velocity is nicely recovered, thus indicating that the velocity extraction by double multipath summation can actually work. However, the velocity model is rather unstable, with many image points where unreliable and wrong velocities have been extracted. These velocities already indicate the necessity to post-process this velocity model in order to extract only the meaningful velocities.

The most obvious way to evaluate the quality of a time-migration velocity model is to use it for time migration. As shown in Figure 5, the velocity model obtained with the stabilized division (already with a rather small $\epsilon \times \operatorname{sgn} V_W$ added to the denominator of equation (6)) does not lead to an acceptable migrated image. Tests with different values for the stabilization parameter did not help to improve the image. The reason is that ungeologically low velocities the time migration cannot deal with are attributed to many locations in the model. These velocity values need to be eliminated by post-processing.

Since nongeological values must not be allowed in the final velocity model, an obvious idea is to already simply avoid division where the absolute value of the denominator is too small (below one half percent of the peak amplitude in a 250 ms window), and also discard velocities that are out of the range of velocities that were actually used for the multipath migration. At all these image points, the velocity is set to zero. Figure 6 shows the result of such a masked division, where zero is attributed to the velocity model wherever the denominator is too small to allow for a division or where unacceptable velocity values result from the division. This eliminates the incorrect velocity values but replaces them by zeroes, thus creating the need for velocity interpolation.

This can be clearly seen from the resulting time migration using this masked velocity model (see Figure 7). In this case, the migration was actually carried out only for those grid points where the velocity is different from zero We see that the migrated image nicely focuses the reflectors in the less complex areas, however creating some holes in the more complex parts.

A simple fill of the missing velocity values by the nearest nonzero neighbor leads to the velocity model shown in Figure 8. This velocity model no longer contains any zeros, but still is not smooth enough to be acceptable as a time

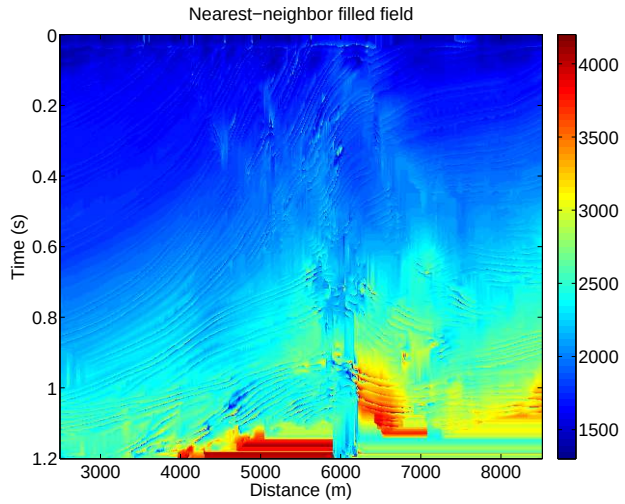

Figure 8: Velocities extracted by masked division plus nearest-neighbor filling.

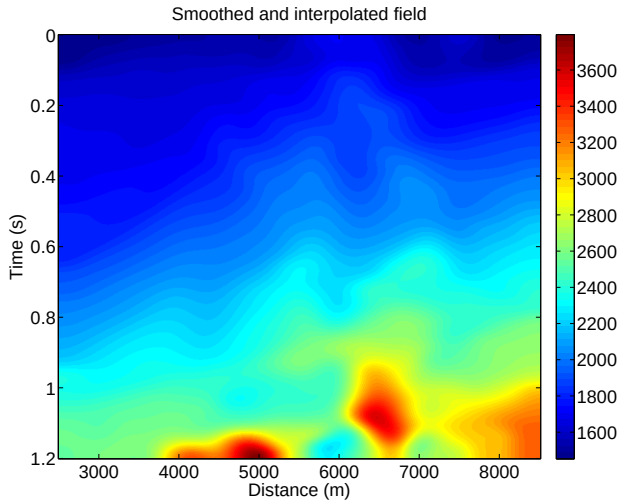

Figure 10: Velocities extracted by masked division plus moving-average smoothing.

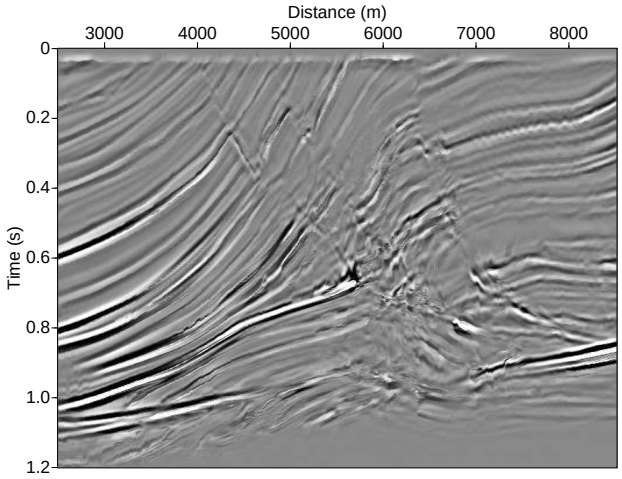

Figure 9: Time migration using velocities extracted by masked division plus nearest-neighbor filling.

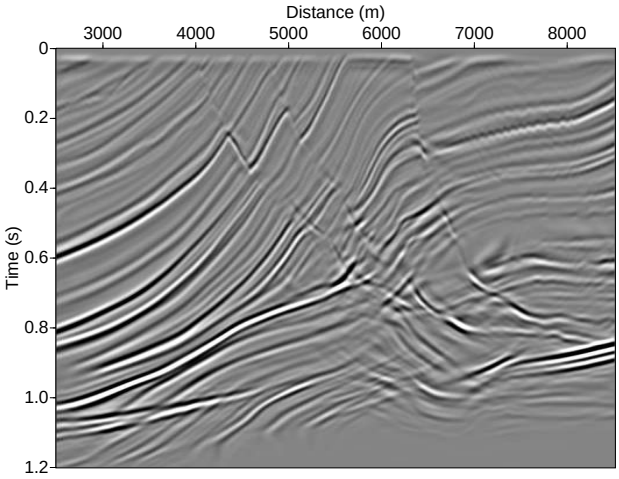

Figure 11: Time migration using velocities extracted by masked division plus moving-average smoothing.

migration velocity model. This can be confirmed from the resulting time-migrated image (Figure 9). The holes in the image have been filled, leading to a complete image. However, the lack of focussing in the central part of the image indicates that there is still room for further improvement.

Since a time-migration velocity model theoretically consist of rms velocities, it is supposed to be smooth. Rather than smoothing the model in Figure 8, we chose to directly smooth the masked model of Figure 6, testing two kinds of smoothing techniques.

First, we applied moving-average smoothing using a window in which zero values of the velocity were ignored. It turned out that passing a smaller window several times yields a more reliable result than passing a larger window only once. Figure 10 depicts the resulting smooth velocity model after four passes of a smoothing window of 25 traces by 17 time samples. Note that the resulting velocity model closely resembles the model constructed with image-wave propagation in the image gather (Schleicher et al., 2008).

The smoothed model considerably increases the image quality in the complex bottom and center parts (Figure 11). While the image is still not perfect in this region, this problem should be attributed to the general limitations of time migration in geologically complex areas rather than taking it as an indication of a poor velocity model.

Another way of obtaining a reasonably smooth time-migration velocity model from the masked velocities in Figure 6 is by B-splines interpolation. In this technique, B-splines coefficients on a regular grid are estimated by regularized least squares using all the available velocity information, neglecting the gaps. The resulting velocity model for a moderate regularization is shown in Figure 12. The velocity model is rather similar to the one obtained with moving-average smoothing (Figure 10). The same applies to the time-migrated image (Figure 13). It is hard to spot significant differences between the two migrated images in Figures 11 and 13. Most of the slight differences that do exist occur in the center part of the model, where the geology is so complicated that time migration cannot realistically be expected to correctly position the reflectors.Note that the time-migrated images in Figures 11 and 13 are very similar to the multipath image of Figure 2, indicating that the extracted velocity model is consistent with the mul-

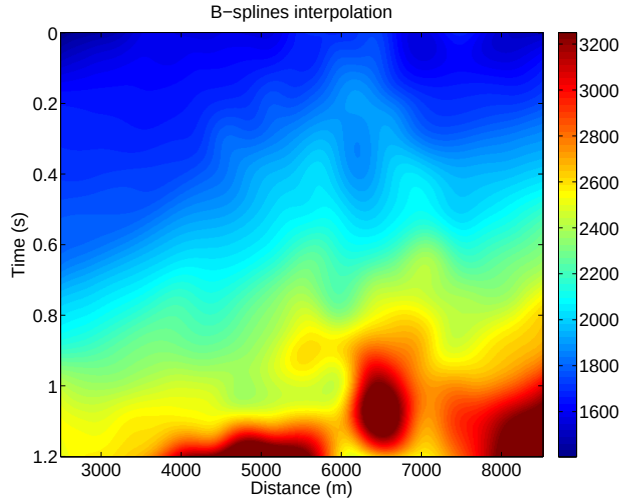

Figure 12: Velocities extracted by masked division plus B-splines smoothing.

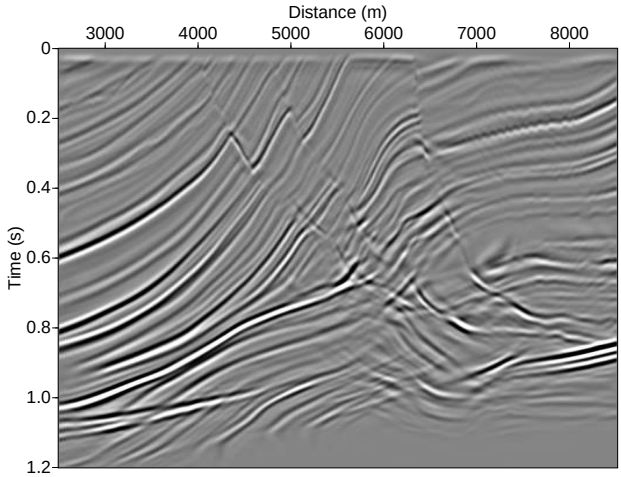

Figure 13: Time migration using velocities extracted by masked division plus B-splines smoothing.

tipath method.

Common-image gathers allow for a more detailed evaluation of the quality of the migration velocity model. Figure 14 shows six common-image gathers at positions 3000 m to 8000 m at every 1000 m in the moving-average smoothed model of Figure 10. We observe that these gathers are flattened in the more regular parts of the model. The method only has difficulties to flatten the gathers in the central part of the model, where the geologic complexity is effectively prohibitive for any kind of time migration. For comparison, Figure 15 show the corresponding image gathers as obtained with the B-splines model of Figure 12. Even in the image gathers, it is very difficult to see differences between the two results.

Implementational Aspects

Let us now discuss some implementational aspects of double multipath migration. First of all, we note that the computational cost of double multipath migration is only slightly higher than for a single multipath migration. All that is needed is the multiplication of the migrated image by the present velocity, a summation into a second, velocity-weighted image, and a division of the final results at each point in the image. The computationally most expensive part, the time migration for each of the chosen velocities, is done only once. The computational cost of a single multipath migration is, of course, N_v times the cost of a single time migration, where N_v is the number of velocities used.

The memory requirements of double multipath migration are also only slightly larger than those of a single multipath migration. The full prestack migrated volume needs only to be saved once. All additional fields needed for double multipath migration have the dimensions of the final stacked image. The memory requirements of single multipath migration are of the order of a conventional prestack migration.

The total cost of the proposed velocity analysis is just the one of double multipath migration. The velocity extraction, interpolation, and smoothing can be done fully automatically, without the need of human interpretation or other intervention.

Conclusions

The idea of path-integral imaging is to sum over the migrated images obtained for a set of migration velocities. Those velocities where common-image gathers align horizontally are stationary, thus favoring these images in the overall stack. Other CIGs cancel each other in the final stack. An exponential weight function using the event slopes in the CIGs helps to enhance the constructive interference and to reduce undesired events that might not be completely canceled by destructive interference.

Evaluation of the resulting path integral with Laplace's method demonstrated that the resulting image is proportional to the image that would be obtained with the correct velocity model. By executing the path-integral imaging a second time with a modified weight function including the migration velocity as an additional factor, an additional image is obtained the amplitudes of which are proportional to the stationary values of the migration velocity. Thus, these stationary velocities that produce the final image can then be extracted by a division of the two images. We have demonstrated with a numerical example that meaningful information about the migration velocity can be extracted from such a double path-integral migration.

Since multipath-summation imaging does not rely on any kind of interpretation, this technique allows for the fully automated construction of a first time-migrated image together with a first time-migration velocity model. This model can then be used as a starting model for subsequent velocity analysis tools like migration velocity analysis or tomographic methods.

It is to be stressed that the proposed velocity extraction technique does not compromise the velocity-independent philosophy. The foremost result of multipath migration continues to be the stacked velocity-independent image. However, with just a few extra operations, a velocity model is obtained as an automatic by-product of the method.

Acknowledgments

We thank Gilles Lambaré and Pascal Podvin for making the Marmousoft data set available to us. This work was

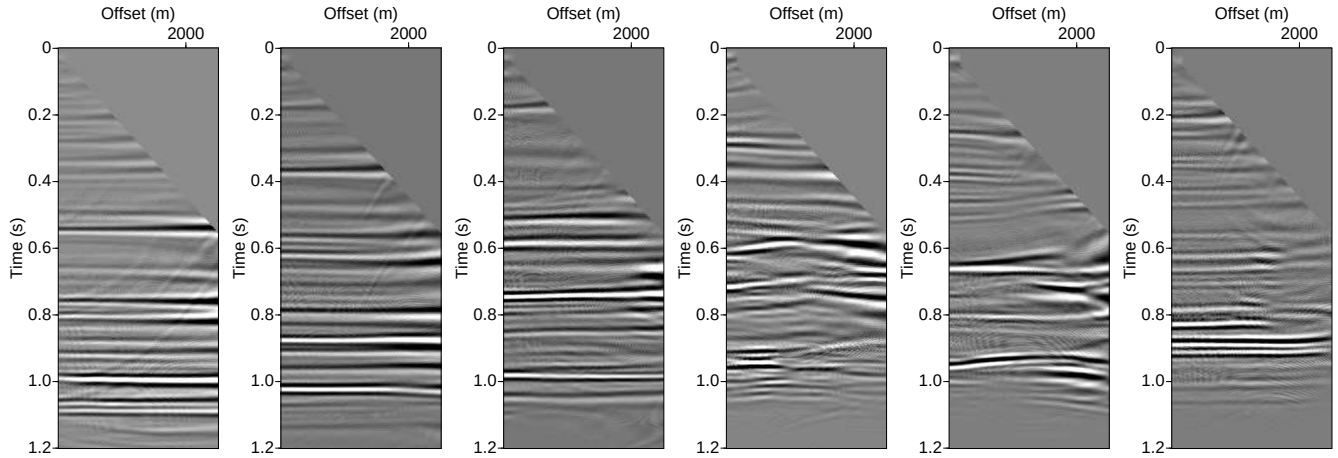

Figure 14: Common-image gathers from time migration using velocities extracted by masked division plus moving-average smoothing. (a) $x = 3000$ m, (b) $x = 4000$ m, (c) $x = 5000$ m, (d) $x = 6000$ m, (e) $x = 7000$ m, (f) $x = 8000$ m.

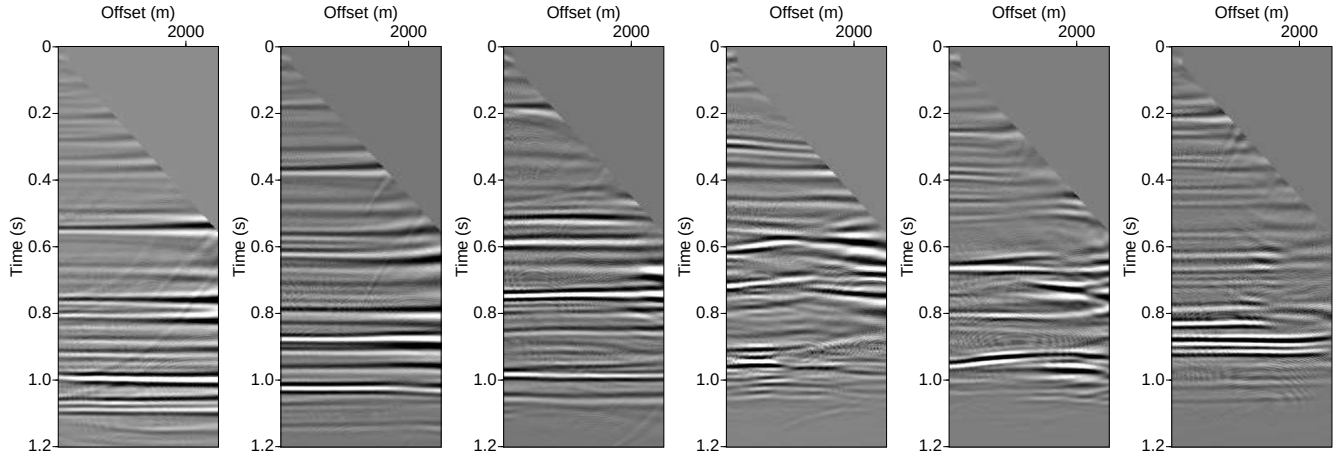

Figure 15: Common-image gathers from time migration using velocities extracted by masked division plus B-splines smoothing. (a) $x = 3000$ m, (b) $x = 4000$ m, (c) $x = 5000$ m, (d) $x = 6000$ m, (e) $x = 7000$ m, (f) $x = 8000$ m.

kindly supported by the Brazilian national research agencies CNPq and CAPES, as well as Petrobras and the sponsors of the *Wave Inversion Technology (WIT) Consortium*.

References

Billette, F., S. Le Bégat, P. Podvin, and L. G., 2003, Pratical aspects and applications of 2d stereotomography: Geophysics, **68**, 1008–1021.

Bleistein, N., 1987, On the imaging of reflectors in the earth: Geophysics, **52**, 931–942.

Keydar, S., 2004, Homeomorphic imaging using path integrals: 66th Annual International Meeting, EAGE, 66th Annual Int. Mtg., EAGE, Expanded Abstracts, P078:1–4.

Keydar, S., V. Shtivelman, M. Milkenberg, and T. J. Moser, 2008, 3D prestack time migration by multipath summation: 70th Annual International Meeting, EAGE, 70th Annual Int. Mtg., EAGE, Expanded Abstracts, P036:1–4.

Landa, E., 2004, Imaging without a velocity model using path-summation approach: 74th Annual International Meeting, 74th Ann. Int. Mtg, SEG, Expanded Abstracts, 1818–1821.

Landa, E., S. Fomel, and T. J. Moser, 2006, Path-integral seismic imaging: Geophysical Prospecting, **54**, 491–503.

Landa, E., M. Reshef, and V. Khaidukov, 2005, Imaging without a velocity model by path-summation approach: This time in depth: 67th Annual International Meeting, EAGE, 67th Annual Int. Mtg., EAGE, Expanded Abstracts, P011:1–4.

Schleicher, J., J. C. Costa, and A. Novais, 2008, Time-migration velocity analysis by image-wave propagation of common-image gathers: Geophysics, **73**, no. 5, VE161–VE171.

Schleicher, J., J. C. Costa, L. T. Santos, A. Novais, and M. Tygel, 2009, On the estimation of local slopes: Geophysics, **74**. (in print).

Shtivelman, V., and S. Keydar, 2005, Imaging shallow subsurface inhomogeneities by 3D multipath diffraction summation: First Break, **23**, 39–42.

Tygel, M., J. Schleicher, P. Hubral, and C. Hanitzsch, 1993, Multiple weights in diffraction stack migration: Geophysics, **58**, 1820–1830.